ACCOUNTS of chemical research

Article

pubs.acs.org/accounts

Kinetics of Iodine-Free Redox Shuttles in Dye-Sensitized Solar Cells: Interfacial Recombination and Dye Regeneration

Zhe Sun,[†,‡] Mao Liang,[†,‡] and Jun Chen*[,†]

[†]Key Laboratory of Advanced Energy Materials Chemistry (KLAEMC) (Ministry of Education) and State Key Laboratory of Elemento-Organic Chemistry, Collaborative Innovation Center of Chemical Science and Engineering, Nankai University, Tianjin 300071, People's Republic of China

[‡]Tianjin Key Laboratory of Organic Solar Cells and Photochemical Conversion, School of Chemistry & Chemical Engineering, Tianjin University of Technology, Tianjin 300384, People's Republic of China

Supporting Information

CONSPECTUS: Dye-sensitized solar cells (DSCs) have gained widespread attentions owing to their low production cost, tunable optical response, and high light-to-electricity conversion. In DSCs, the performance of redox mediators with iodide/triiodide or iodine-free redox couples is vital to internal quantum efficiency. For a long time, iodide/triiodide based electrolytes are the most widely used mediators because of their desirable kinetics. Recently, exciting progress has been made with respect to iodine-free metallorganic and pure organic redox shuttles. Their tunable redox potential and diverse electron transfer behaviors enable the rational screening of electrolyte composition for enhancing the light-to-electricity conversion efficiency of DSCs toward the Shockley–Queisser limit. In this Account, we emphasize on current knowledge of two distinct but interrelated interfacial processes (electron recombination and dye regeneration), particularly for DSCs with iodine-free redox couples. We show that a deeper understanding of electron transfer kinetics of the alternative redox couples is fundamental to develop rational strategies for cell optimization. Compared with iodine electrolyte, iodine-free metallorganic redox couples such as iron, cobalt, and nickel complexes display much faster electron transfer kinetics in dye regeneration and interfacial recombination. Evidently, rapid regeneration enables the employment of more positive metal complex for attaining a higher photovoltage. However, severe recombination reactions have to be well controlled by using several effective surface treatments such as the addition of Brönsted bases and atomic layer deposition. Although these methods offer different pathways in surface passivation, a trade-off between charge injection efficiency and electron diffusion length is always observed. It follows that an appropriate LUMO level of sensitizer is essential to ensure efficient electron injection at the passivated TiO_2 surface. Apart from fast recombination behavior, bulky metal complexes suffer from inefficient charge transport. Thus, the combination of thinner TiO_2 film and sensitizers with high mole extinction coefficient has been employed for both enhancing diffusion-limited current and maintaining light-harvesting efficiency. Unlike metal complexes, most of organic sulfur redox couples in DSCs exhibit slow recombination kinetics. This allows the use of thicker TiO_2 film to achieve an optimized light harvesting. However, the concomitant sluggish behavior of dye regeneration requires the use of sensitizers with more positive HOMO level, which is beneficial to efficient regeneration. Moreover, lower level of TiO_2 band edge in DSCs based on organic sulfur mediators hinders the achievement of desirable photovoltage, spurring future explorations on this class of redox mediator.

Based on the comparison of electron transfer behavior between iodine-free metallorganic complexes and pure organic redox couples, we aim to provide a comprehensive Account of the intriguing interfacial processes in iodine-free DSCs as the key scientific point is linked with the kinetics of interfacial reactions. This demonstrates the advantages as well as disadvantages of each class of iodine-free electrolyte and should shed light on to judicious selection of the energy levels for redox mediators, sensitizers, and the conduction band of TiO_2 for DSCs. The knowledge of the reaction kinetics in DSCs should be also beneficial to the interface engineering on recent developed perovskite cells.

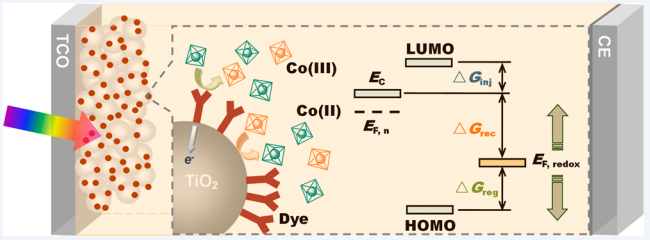

1. INTRODUCTION

Dye-sensitized solar cells (DSCs) have attracted persisting interest for their advantages of wide range selectivity in light adsorption, excellent photovoltaic performance, and easy application in flexible modules.[1,2] The operation of DSCs is depicted as an energy conversion network constituted by a variety of interfacial reactions, as shown in Figure 1. In particular, DSCs can be viewed as an intriguing model for scrutinizing the kinetics of interfacial electron transfer in a nanoporous framework of metal oxides. Obviously, the knowledge of these reactions is a guideline for improving interfacial charge

Received: May 18, 2014
Published: May 22, 2015

DOI: 10.1021/ar500337g
Acc. Chem. Res. 2015, 48, 1541−1550

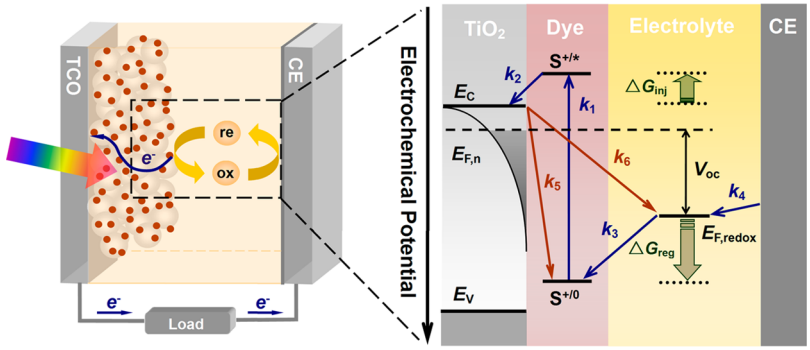

Figure 1. Schematic composition of an operating DSC (left). Reactions occurring within the dashed rectangle are illuminated as an energy diagram (right): k_1, excitation of the sensitizers; k_2, electron injection; k_3, regeneration of the sensitizers; k_4, electron transfer at cathode; k_5, recombination with the oxidized sensitizers; k_6, recombination with the oxidized form of redox couple.

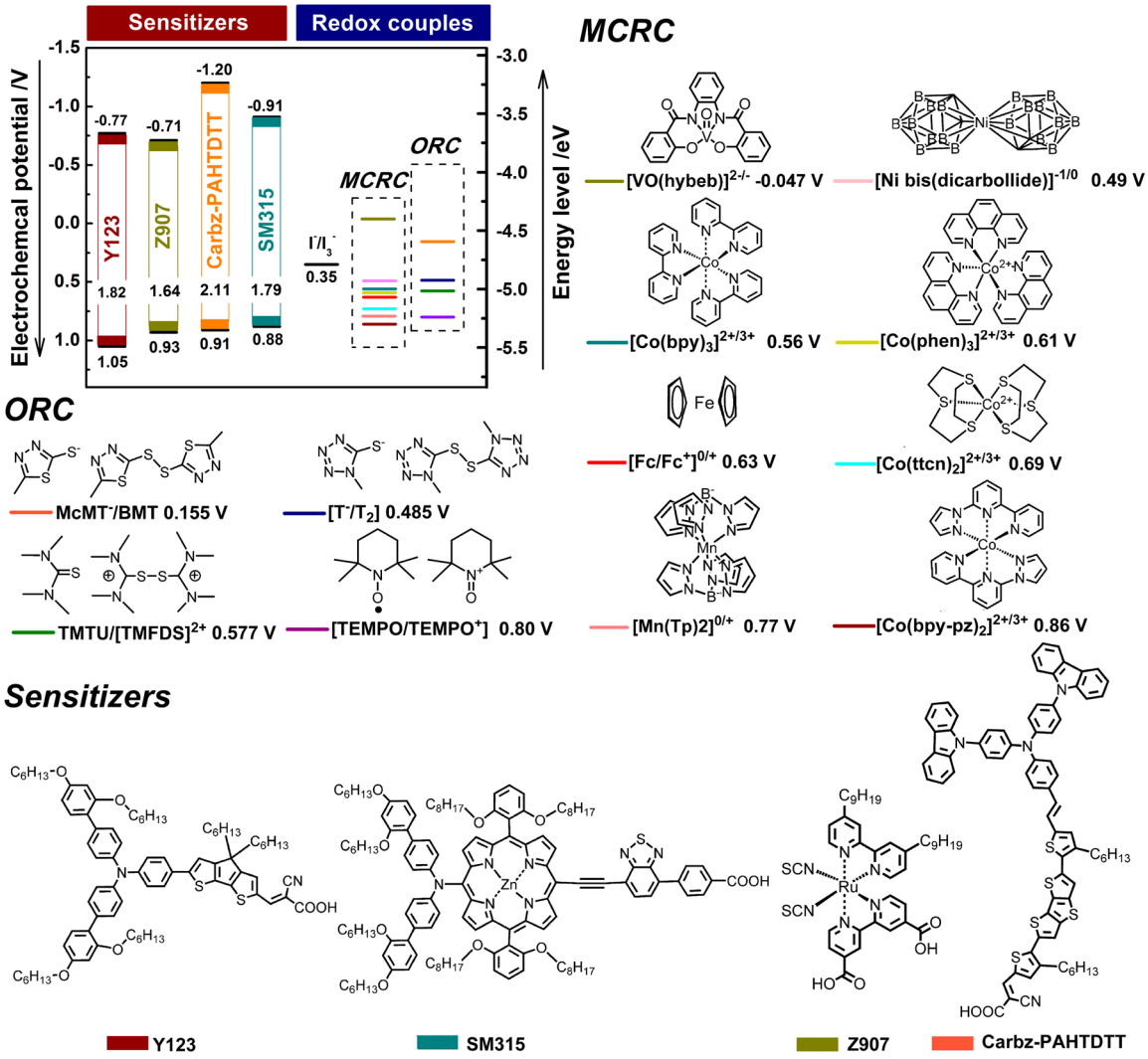

Figure 2. Schematic energy diagrams of selected sensitizers, metal complex redox couples (MCRC), and organic redox couples (ORC). Redox potential of redox couples and sensitizers is indicated relative to normal hydrogen electrode (NHE). Energy levels are based on the electrochemical scale (NHE) which is taken at −4.4 eV.

separation in both DSCs and even recent perovskite devices, in which the former has an insulating dye monolayer whereas the latter is equipped with conductive organometal halide crystals.

Considerable efforts have long been devoted to explore alternative redox couples in place of iodine based electrolyte which is known for its high overpotential (>0.6 V) in dye regeneration, visible light absorption, and undesirable recombination owing to dye-I_2 binding. Recently, a variety of promising iodine-free electrolytes including metallorganic and organic sulfur redox mediators have been developed. A salient feature of such iodine-free redox couples is their adjustable molecular architectures, which helps to realize a fine-tuning of redox

DOI: 10.1021/ar500337g
Acc. Chem. Res. 2015, 48, 1541−1550

potential (Figure 2) as well as an improvement of operating stability. It is notable that DSCs fabricated with cobalt-based redox couple $[Co(bpy)_3]^{2+/3+}$ and Zn-porphyrin sensitizer SM315 have demonstrated a power conversion effeciency (PCE) of 13%, setting a new benchmark for DSCs.[3] Nevertheless, there remains much scope to improve device performance. Snaith suggested the efficiency of DSC will reach to 20.25% if the energy losses in DSCs are properly reduced and the adsorption onset of sensitizer is made to 940 nm.[4] The energy losses primarily originate from the excess overpotential of dye regeneraion, severe interfacial recombination, and the wide optical bandgap of sensitizer. Regarding the issue of redox mediators, energy losses are highly relative to the redox potential, electron transfer behaviors, and even the chemical property of electrolyte. It is common for metallorganic redox couples to exhibit recombination rate faster than I^-/I_3^- by 2−3 orders of magnitude, leading to a loss in voltage by 116−174 mV and dramatic drop of photocurrent by 25.8−68.5% for an ideal DSC (see the Supporting Information). Interestingly, those redox couples featuring fast recombination kinetics usually regenerate the dye cations more efficiently. This means that less driving force is required to maintain quantitative regeneration of dye cations, which enables the employment of the sensitizers with narrower optical bandgap. Meanwhile, the alternation of redox couple induces a change of chemical circumstance surrounding TiO_2 nanoparticles and hence shifts the conduction band (CB). Special treatments to TiO_2 photocathode are thus required to locate the CB edge at an appropriate level. Overall, the variation of redox rouple results in a systematic change of electron transfer behavior and energy-level alignment in DSCs. Thereby, the LUMO and HOMO levels of sensitizers, the band edge level, and even the pathway of surface passivation should be designed accordingly.

This Account highlights the representative electron transfer kinetics of recent explored metallorganic and organic sulfur redox couples. We further illuminate several effective protocols for handling the intriguing electron transfer behaviors. Additionally, the relation between electron transfer kinetics and energy engineering of iodine-free cells is also addressed.

2. INTERFACIAL RECOMBINATION

2.1. Metallorganic Redox Couples versus Organic Sulfur Redox Couples

2.1.1. Cobalt Based Redox Couples. The most successful metallorganic redox couples to date are cobalt polypyridyl complexes. The large activation barrier for spin changes from Co(III) to Co(II) renders these redox mediators relatively sluggish kinetics of electron interception.[5] So it is easy to realize a fine-control of the recombination in cobalt-complex based DSCs. However, there is no denying that the electron interception of cobalt complexes is still much faster than I^-/I_3^-. For this reason, electron lifetime and charge collection efficiency for cobalt-complex based DSCs were usually shown at a low value in the earlier studies. Progress has been made by employing insulating alkoxyl chain decorated sensitizers and *tert*-butylpyridine (TBP) contained electrolyte for impeding recombination (Figure 3).[5] With this strategy, charge collection efficiency has exceeded 90% as Yum et al. reported.[6] Wang's group demonstrated that $[Co(phen)_3]^{2+/3+}$ based cells give 100 mV higher V_{oc} than the iodine counterpart. In view of more positive redox potential of $[Co(phen)_3]^{2+/3+}$ by 140 mV, one can estimate a lower voltage loss of 40 mV in the cobalt cells.[7] Even so, the remaining

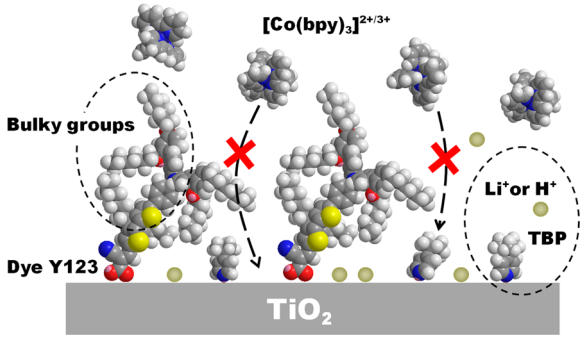

Figure 3. Schematic of the recombination reactions retarded by organic dye Y123 and additives at cobalt-based electrolyte/TiO_2 interface.

photovoltage loss implies that a part of the gain in voltage by using $[Co(phen)_3]^{2+/3+}$ with more positive redox potential is inevitably compesated by the fast dynamics of electron interception. Moreover, large molecular size of cobalt complexes is known to render inefficient charge transport in DSCs and hence limit the output of photocurrent. An effective solution proposed by Boschloo and co-workers is to utilize a thinner TiO_2 film (2−5 μm) for enhancing diffusion limited current.[5] Note that sensitizers with high mole extinction coefficient are necessary for the devices to attain efficient light harvesting.

One of the advantages of cobalt complexes is their tunable redox potential by varying the ligand. This allows the Co(III) complex with proper energy level to serve as p-dopant in solid-state DSCs based on spiro-MeOTAD.[8] Such chemical p-doping was shown to improve hole-conductivity and device stability simultaneously. Moreover, the potential tunability of cobalt complexes helps to uncover the dependence of electron interception kinetics on the energy-level of redox couples. Feldt et al. showed that cobalt complexes in liquid-state DSCs prefer to react with the electrons at the conduction band rather than the band gap states.[9] Reorganization energy λ of interfacial recombination is estimated as 1.05 eV. As shown in Figure 4, the

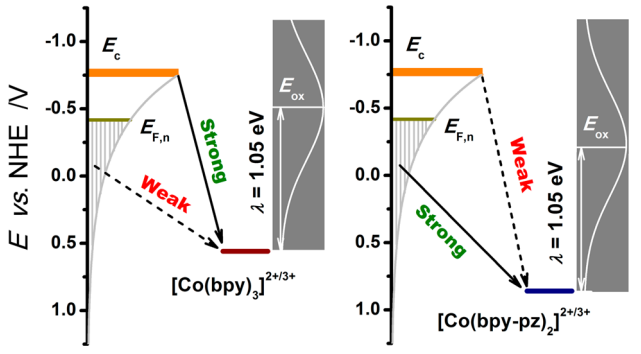

Figure 4. Schematic recombination kinetics of cobalt-complex redox couples. The light gray domains below the Fermi-level mark the occupied bandgap states. Data of reorganization energy are obtained from ref 9.

energy level of Co(III) complex matches well with the conduction band instead of the surface states. Only when redox potential of cobalt complexes exceeds 0.85 V, does the recombination via the surface states become significant. The electron interception appears to fall in the Marcus inverted region when redox potential of cobalt complexes is over ~0.56 V. Theoretically, it implies that the recombination rate constant could be reduced by employing cobalt complexes with more

DOI: 10.1021/ar500337g
Acc. Chem. Res. 2015, 48, 1541−1550

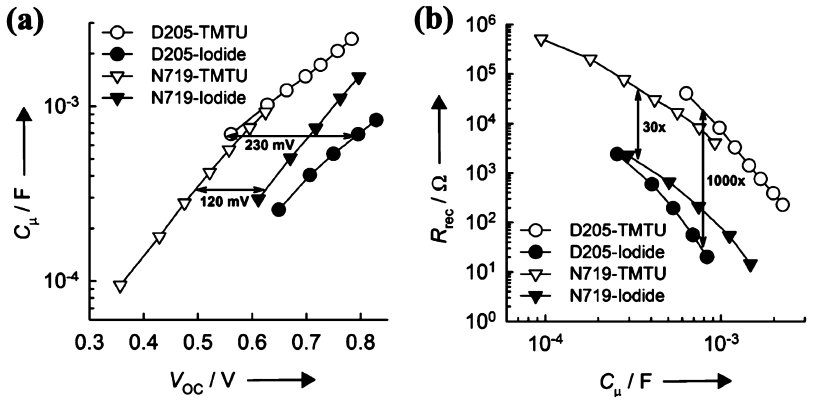

Figure 5. Plots of (a) capacitance versus photovoltage (C_μ–V_{oc}) and (b) recombination resistance versus capacitance (R_{rec}–C_μ) for devices sensitized by D205 and N719 dyes in the presence of TMTU-based and iodide-based electrolytes. Images are reprinted from ref 17 with permission from Wiley.

positive potential or just shifting the band edge negatively. However, this validity needs to be scrutinized because the recombination behavior is severely affected by solvent and additives surrounding the titania/electrolyte interfaces.

2.1.2. Iron Based Redox Couples. Ferrocene/ferrocenium (Fc/Fc^+) redox couple has been demonstrated as an interesting electrolyte candidate with more positive potential relative to I^-/I_3^-. The self-exchange rate of Fc/Fc^+ is larger than that of iodide/triiodide ($\sim 2 \times 10^5$ M^{-1} s^{-1}) by 2 orders of magnitude, being $\sim 10^7$ M^{-1} s^{-1}.[10] So far the most effective protocol dealing with ultrafast recombination is to utilize thinner film with the thickness ranging from several micrometers to a few hundreds of nanometers. Upon this method, the distance of electron diffusion to FTO glass and the number of surface defects of TiO_2 are reduced simultaneously. Such strategy is also applicable to solid-state DSCs and perovskite-based devices.

Bach and co-workers achieved an efficiency boost of iron-based cells by performing a systematic design on device components and careful exclusion of oxygen from electrolyte due to the instability of ferrocenium.[11] A novel organic dye (Carbz-PAHTDTT) in combination with the coadsorbent chenodeoxycholic acid (CDCA) affords the yielded V_{oc} of 842 mV and PCE of 7.5% for Fc/Fc^+ based devices. Although thinner film is critical to the improvement of cell performance, Bisquert argued that it could not account for the 100 mV increment of V_{oc} when replacing I^-/I_3^- with Fc/Fc^+.[12] He ascribed the V_{oc} increase to higher level of the band edge. For the studied DSCs, the variation of redox potential is 270 mV, while the contribution from the negative band edge shift is about 190 mV. In principle, the gain in voltage should be 460 mV, sharply contrasting a 100 mV enhancement as observed. Evidently, there is a 360 mV loss in voltage as a result of the ultrafast recombination of Fc/Fc^+.

Bisquert suggested that high LUMO level of Carbz-PAHTDTT (−1.20 V vs NHE, Figure 2) is ultimate to the increase of V_{oc} without significant loss of photocurrent because this level brings forth to a sufficient driving force for electron injection at a high band edge level.[12] Unfortunately, Carbz-PAHTDTT exhibits a wide band gap of 2.11 eV (Figure 2), which limits light harvesting in the near-infrared part of solar spectrum.

2.1.3. Nickel, Manganese, and Oxidovanadium Based Redox Couples. One-electron outer-sphere Ni(III)/(IV) bis(dicarbollide) shows interesting kinetics of electron interception.[13] A conformation change from *cis* to *trans* during the reduction of Ni (IV) to Ni(III) allows the electron interception rate in the DSCs 1000 times slower than that in Fc/Fc^+ cells. Similarly, Mn(II)/(III) poly(pyrazolyl)borates (e.g., $[Mn(Tp)_2]^{+/0}$) were recently been examined due to their kinetic barrier from a low-to-high spin transition (t_{2g}^4 Mn(III) → $t_{2g}^3e_g^2$ Mn(II)).[14] Resultantly, a lower heterogeneous electron transfer rate ($[Mn(Tp)_2]^{0/+}$ 1×10^{-4} cm s^{-1} vs. $Fc^{0/+}$ 1 cm s^{-1}) affords the decreased recombination. By contrast, oxidovanadium(IV/V) complexes ($[VO(hybeb)]^{2-/-}$) display fast electron interception (self-exchange rate exceeding 10^9 M^{-1} s^{-1}).[15] Not surprisingly, substantial photocurrent loss is observed when using dye N719 in the oxidovanadium complex based DSCs. It implies that the protocol of using high mole extinction coefficient sensitizer with coadsorbent will be helpful for improving cell efficiency.

2.1.4. Organic Sulfur Redox Couples. Due to the transparent and noncorrosive nature, organic sulfur redox couples have been proposed as valuable alternative mediators. Recently, Wang et al. presented a new disulfide/thiolate (T^-/T_2) redox couple showing a device efficiency of 6.4%.[16] In contrast to fast one-electron organic redox shuttles (TEMPO/$TEMPO^+$), two-electron redox couple T^-/T_2 displays sluggish electron interception.[16] Notably, the electron lifetime of the T^-/T_2 device is even longer than that of iodine-based DSC by approximately 25-fold, indicating that the gain in voltage from lower recombination rate is ∼80 mV. However, the CB edge of the T^-/T_2 device is significantly lower than that of the iodine cell by ∼225 mV, which heavily limits the V_{oc} of the T^-/T_2 device (696 mV).

Electron interception kinetics in the tetramethylthiourea/tetramethylformaminium disulfide (TMTU/$[TMFDS]^{2+}$) is similar to the T^-/T_2 system. As presented in Figure 5, the recombination rate of TMTU/$[TMFDS]^{2+}$ in the devices of indoline dye D205 is 1000-fold slower than the iodine counterpart, corresponding to a gain in potential of ∼175 mV.[17] Despite the significantly attenuated recombination, the photovoltage of the TMTU/$[TMFDS]^{2+}$ cell (0.777 V) is still below the iodine cell (0.801 V). With the aid of impendence techniques, Wang and co-workers attributed this to the fact that TMTU/$[TMFDS]^{2+}$ cell shows ∼430 mV more positive level of the band edge compared with iodine DSC. Note that similar trends in recombination and CB shift occurred in N719-sensitized DSCs. However, the V_{oc} of this device is ∼150 mV lower than that with D205. This could be ascribed to the inefficient regeneration of dye cations.

Interestingly, another organic sulfur redox couple of $McMT^-$/BMT has a different effect on the CB edge in DSCs. This redox

DOI: 10.1021/ar500337g
Acc. Chem. Res. 2015, 48, 1541−1550

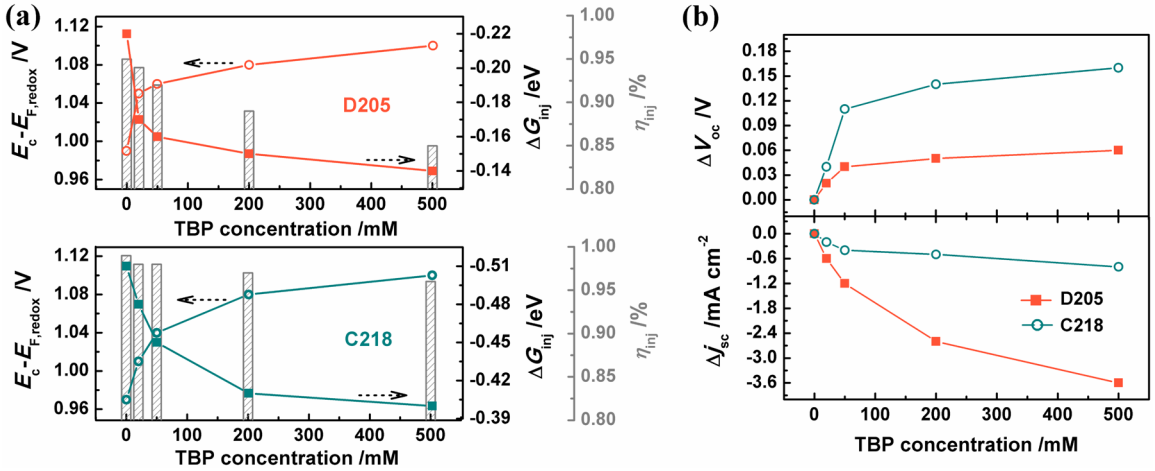

Figure 6. (a) Plots of the relative conduction band edge (E_c–$E_{F,redox}$), driving force of injection (ΔG_{inj}), and injection efficiency (η_{inj}) versus TBP concentration. (b) Effects of TBP concentration on the changes of open circuit voltage (ΔV_{oc}) and short circuit current density (Δj_{sc}). Sensitizers D205 and C218 show LUMO levels of −1.22 and −1.49 V vs NHE, respectively. Experimental data for the plots are attained from ref 21 with permission from American Chemical Society.

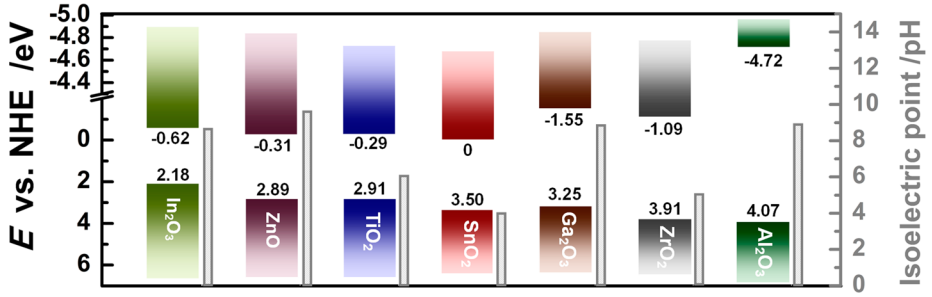

Figure 7. Band gap and isoelectric point of various metal oxides.

couple causes a significantly negative shift of the CB edge by 100 mV.[18] The employing of McMT$^-$/BMT redox couple is also found to significantly decrease the interfacial recombination rate (about 10 times slower than I^-/I_3^-). These two beneficial factors can compensate the loss of V_{oc} from the upward shift of redox potential, which was estimated to be 0.155 V vs NHE.

Evidence from the cited works shown above clearly demonstrates the advantage of sluggish recombination of the organic sulfur redox couples in photovoltage. Thereby, a rational choice is to employ thicker TiO_2 film (~10 μm) for attaining an optimal light-harvesting and hence a comparable photocurrent with respect to the iodine cell.

2.2. Modification of TiO_2/Electrolyte Interface

2.2.1. Effects of Additives. The introduction of Brönsted bases such as *N*-methylbenzimidazole (NMBI), *tert*-butylpyridine (TBP) and other relative pyridine derivatives into electrolyte solution has been demonstrated as a powerful tool for minimizing the unfavorable recombination (Figure 3) and tuning the CB edge. Several possible mechanisms including the occupation of TBP on the oxygen vacancies at TiO_2 surface, proton-binding, or the substitution of the adsorbed protons and/or Li^+ have been proposed for explaining the blocking effect.[19] Such mechanisms are mutually compatible and consistent with the experimental observations, showing that the presence of TBP leads to the decrease of recombination rate constant, the negative shift of the band edge, and deeper distribution of the bandgap states.

Many works have demonstrated that the influence of TBP on V_{oc} in the DSCs with cobalt complexes is similar to the behaviors of iodine-based devices. However, Han and co-workers uncovered the shielding effect of TBP on $[Co(bpy)_3]^{2+/3+}$ via weak ion−dipole attractions. Resultantly, the enhancement of V_{oc} is more evident in cobalt-based devices by varying TBP concentration.[20] Also, it is instructive to show the variations of j_{sc} to the TBP concentration demonstrated by Wang's group.[21] Although the data were collected from iodine-based devices, the underlying mechanism is also applicable to iodine-free cells. As presented in Figure 6a, the addition of TBP results in similar movements of the conduction band in DSCs with organic dyes D205 and C218. However, dye C218 has a higher LUMO of 270 mV over dye D205. It follows that the driving force of injection for C218 is sufficient after TBP addition. By contrast, a sharp decrease of electron injection efficiency occurs in the DSCs based on D205. As a result, Figure 6b further displays the apparent decrease of photocurrent in the devices with D205, while less photocurrent loss in combination with the increase of V_{oc} is observed for the devices with C218.

For DSCs with metal-complex redox couples, TBP is also employed extensively to offset the unexpected band edge movement from the introduction of Li+. However, the effect of TBP is quite limited in DSCs employing T^-/T_2 or TMTU/$[TMFDS]^{2+}$.[16] Wang suggested that the presence of lithium ions in TMTU/$[TMFDS]^{2+}$ based devices causes a large downward band edge shift (about 300−400 meV) relative to iodine cells although TBP is employed.[17] If this holds true, the alkalinity of TBP may not strong enough in this system. Thereby, stronger

DOI: 10.1021/ar500337g
Acc. Chem. Res. 2015, 48, 1541−1550

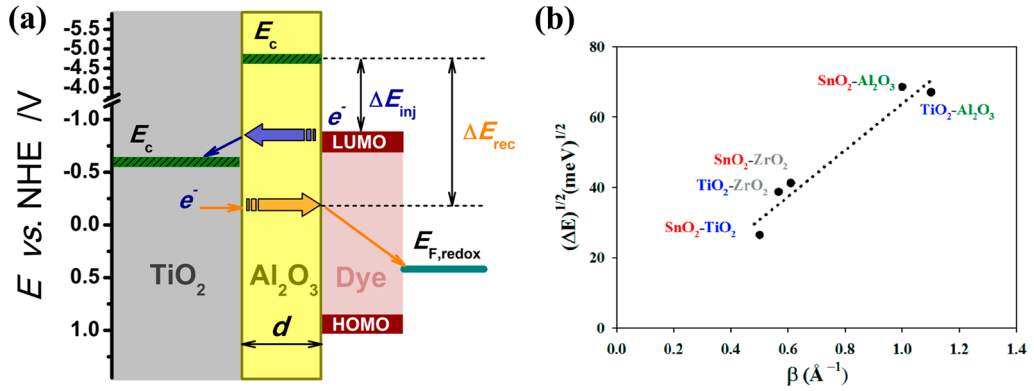

Figure 8. (a) Schematic of electron tunneling through Al_2O_3 layer on a TiO_2 photoelectrode in contact with a solution containing an electron acceptor. (b) Plot of barrier height ΔE against tunneling parameter β. Image (b) is reprinted with permission from ref 25. Copyright 2013 American Chemical Society.

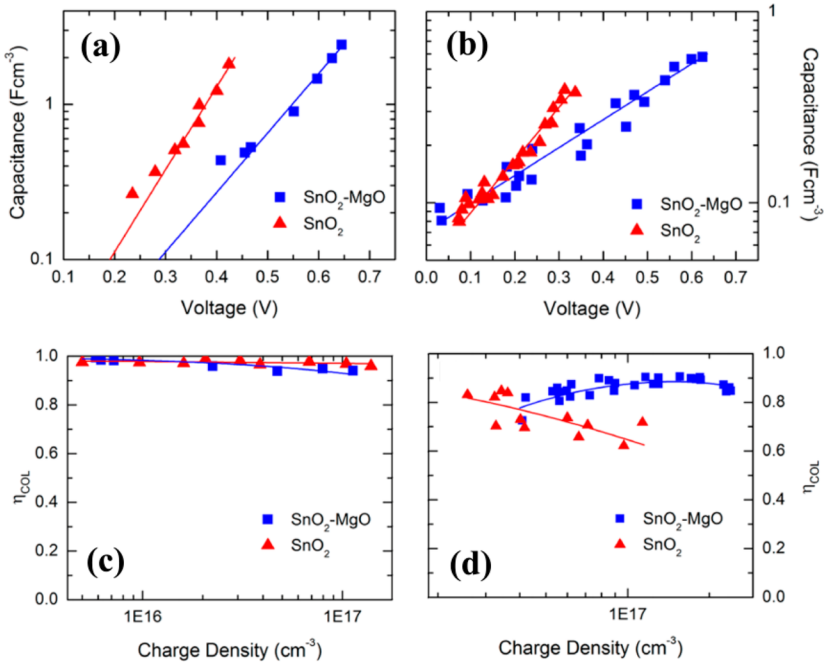

Figure 9. Plots of capacitance versus voltage (a, b) and plots of charge collection efficiencies (η_{COL}) versus charge density (c, d) in DSCs based bare SnO_2 and MgO-coated SnO_2. Images (a) and (c) are depicted for the devices with liquid iodine electrolyte, while images (b) and (d) belong to the solid devices with hole-transport material Spiro-OMeTAD. Images are reprinted with permission from ref 27. Copyright 2012 American Chemical Society.

Brönsted bases like 4-*N*,*N*-dimethylaminopyridine could be an alternative candidate for tuning the CB edge. Meanwhie, we consider that the disulfide cations $[TMFDS]^{2+}$ may play a role in displacing the band edge downwardly by interacting with the TiO_2 surface. To answer these questions, more groundwork is needed.

2.2.2. The Dependence of Interfacial Recombination on Atomic Layer Deposition. Surface passivation for blocking recombination reaction has also been realized by depositing metal oxide films atop the photoanode. In this scenario, atomic layer deposition (ALD) technique is superior to the traditional chemical bath deposition in producing robust and relative uniform shells at the scale of Ångstrom.[22] The functioning of ALD layer in DSCs is affected by its isoelectric point (IEP) and band gap (E_g). A higher IEP is beneficial to the adsorption of sensitizers, while wide band gap helps to shield the electron transfer via the bandgap states. Herein, we present the experimental data of IEP and E_g for most reported metal oxides in Figure 7.

Among these candidates, Al_2O_3 is promising for its wide E_g of ~8.8 eV and desirable IEP of ~pH 9.2. Less than three ALD cycles are sufficient for most ALD-treated DSCs to yield a maximal efficiency (usually below 6%). However, the deposition of Al_2O_3 has been demonstrated in a mode of island growth at the first few ALD cycles.[23] This indicates that lower efficiency could be partly caused by the imperfect surface coverage. For this reason, Chandiran et al. employed Ga_2O_3 for generating conformal ALD layers.[24] It was found that a single ALD cycle engenders over 300 mV increment of V_{oc} in DSC with $[Co(bpy\text{-}pz)_2]^{2+/3+}$ although the E_g of Ga_2O_3 is lower than that of Al_2O_3 by ~3.2 eV. However, their photocurrent results indicate that lower efficiency of ALD-treated DSC is essentially attributed to inefficient electron injection rather than the deficiency of surface covering.

DOI: 10.1021/ar500337g
Acc. Chem. Res. 2015, 48, 1541−1550

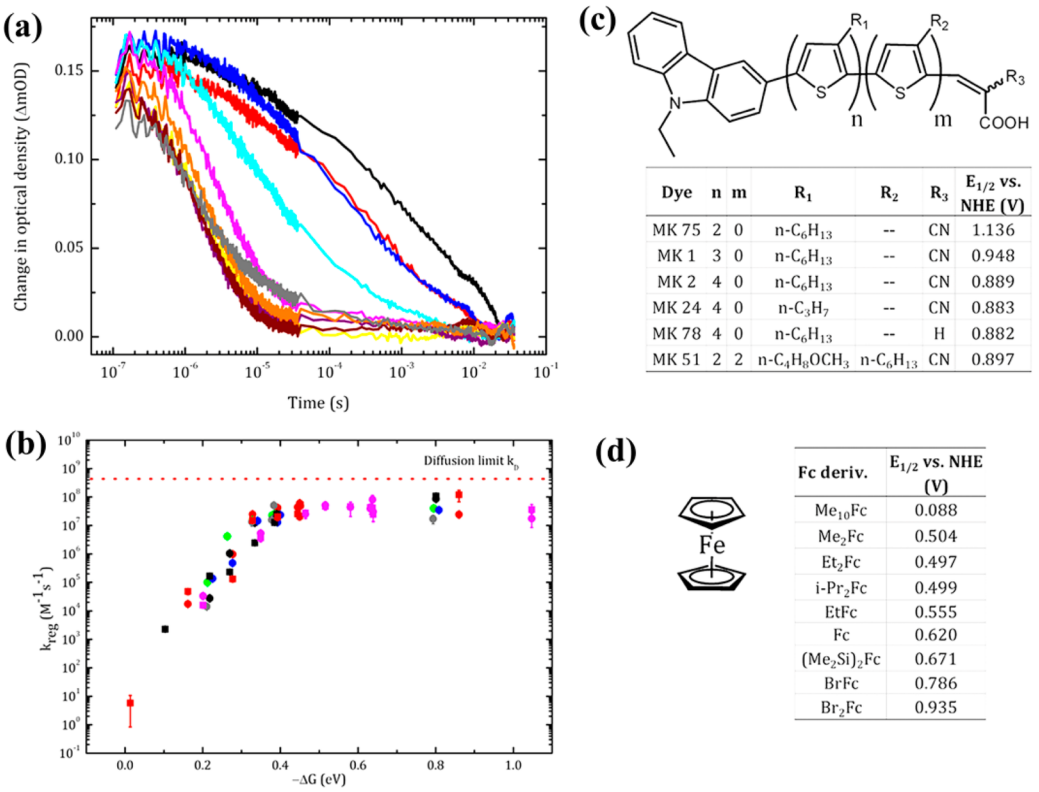

Dye	n	m	R_1	R_2	R_3	$E_{1/2}$ vs. NHE (V)
MK 75	2	0	n-C_6H_{13}	--	CN	1.136
MK 1	3	0	n-C_6H_{13}	--	CN	0.948
MK 2	4	0	n-C_6H_{13}	--	CN	0.889
MK 24	4	0	n-C_3H_7	--	CN	0.883
MK 78	4	0	n-C_6H_{13}	--	H	0.882
MK 51	2	2	n-$C_4H_8OCH_3$	n-C_6H_{13}	CN	0.897

Fc deriv.	$E_{1/2}$ vs. NHE (V)
$Me_{10}Fc$	0.088
Me_2Fc	0.504
Et_2Fc	0.497
i-Pr_2Fc	0.499
EtFc	0.555
Fc	0.620
$(Me_2Si)_2Fc$	0.671
BrFc	0.786
Br_2Fc	0.935

Figure 10. (a) Transient absorbance decays (ΔmOD) for devices using carbazole-based dye MK1 with inert electrolyte (black) and Br_2Fc (red), BrFc (blue), $(Me_2Si)_2Fc$ (cyan), Fc(pink), EtFc (yellow), Me_2Fc (purple), Et_2Fc (wine), iPr_2Fc (orange), and $Me_{10}Fc$ (gray) based electrolytes. (b) Plots of regeneration rate constant k_{reg} versus driving force ΔG for MK1 (red), MK2 (black), MK24 (green), MK51 (blue), MK75 (pink), and MK78 (gray) with ferrocene derivatives. Redox potential for the dyes (c) and the ferrocene derivatives (d). Images are reprinted with permission from ref 30. Copyright 2012 American Chemical Society.

The mechanism underlying the charge transfer across deposition layer was well-described by a barrier tunneling model (Figure 8a),[25] which shows an exponential decay of electron transfer rate constant k_{et} with the thickness of deposition layer d:

$$k_{et} \propto e^{-\beta d} \quad (1)$$

where the tunneling parameter β is scaled as $\Delta E^{0.5}$. The barrier height ΔE is defined as the difference of CB level between the mesoporous matrix and the ALD layer. Figure 8b strongly indicates the dependence of electron tunneling kinetics on the barrier height. This plot not only highlights the validity of Al_2O_3 in blocking recombination but also implies the shortage of that material in electron injection. In practice, the inefficient injection can also be explained as the weakening of electronic coupling between sensitizer and TiO_2.[26] No matter which mechanism is dominant, a trade-off between gain in voltage and loss in photocurrent is unavoidable. Moreover, ALD treatment is not likely to engender a new record of cell efficiency even the components in DSC are fully optimized. It is easy-understood since photocurrent decreases exponentially with d whereas the gain in voltage is only linear to that. Anyway, ALD method is apparently suitable to DSCs with redox mediators or hole transport materials suffering from rapid recombination kinetics, but less helpful to the devices with I_3^-/I^-or organic sulfur redox couples.

It is worthwhile to note that the deposition of Al_2O_3 has no effect on the conduction band and the bandgap states. Interfacial electron transfer could be simply governed by the tunneling mechanism. In contrast, the coating of MgO on SnO_2 was reported to exhibit a negative displacement of the CB edge and a concomitant deeper distribution of the bandgap states.[27] As displayed in Figure 9, this phenomenon is more apparent in Spiro-OMeTAD based DSCs showing a severe interfacial recombination. Similar trends were also observed in In_2O_3-deposited TiO_2 film. Within 20 ALD cycles, the upward band edge shift could be ascribed to the effect of surface dipole.[28]

3. DYE REGENERATION

3.1. Driving Force and Regeneration Efficiency

Efficient regeneration of the oxidized sensitizers is ultimate to the conversion of absorbed incident light to photocurrent in DSCs. To achieve quantitative regeneration, sufficient driving force is required to ensure the reduction rate of the sensitizer cations that exceeds over the rate of the competitive recombination by at least 2 orders of magnitude. As noted before, the existence of overpotential implies a loss in photovoltage. Thereby, rational selection of the potential of redox couple requires a priori knowledge of the threshold of driving force.

Regeneration efficiency (η_{reg}) is a valuable factor for determining the minimal driving force. Usually, η_{reg} is definded as the ratio of regeneration rate to the overall charge transfer rate of the oxidized sensitizers,

$$\eta_{reg} = \frac{k_{reg} n_{RE}}{k_{reg} n_{RE} + k_{rec,S} n_e^{\chi}} \quad (2)$$

DOI: 10.1021/ar500337g
Acc. Chem. Res. 2015, 48, 1541−1550

where n_{RE} is the concentration of the reduced component of redox couple, n_e is the density of the injected electrons, χ is the order of the back reaction with the injected electrons, and k_{reg} and $k_{rec,S}$ represent the reaction rate constants for regeneration and recombination, respectively. In contrast to the linear characteristics of regeneration reaction, the recombination order χ is shown to derivate from unity in iodine-based DSCs by using nanosecond transient absorption spectroscopy (TAS) technique. This result could be reasonably attributed to the electron transfer via various bandgap states. Although the value of χ for iodine-free DSCs is lacking so far, investigations on inert cell revealed that χ is relative to the composition of electrolyte.[29] This implies that the recombination kinetics is affected by the interaction between redox couple and sensitizers or TiO_2 surfaces. Nevertheless, χ could be regarded as an apparent parameter, reflecting the dependence of the recombination rate of dye cations on the Fermi-level of TiO_2. When DSCs are operating near the maximum power point or at open circuit, cell performance could be quite limited by inefficient regeneration.[29]

3.2. Regeneration Kinetics for Iodine-Free Redox Couples

Rapid electron transfer kinetics of ferrocene/ferrocenium (Fc/Fc^+) as mentioned above allows a lower driving force to ensure quantitative regeneration. This means that the voltage loss in dye regeneration could be decreased significantly. Daeneke et al. combined several carbazole-based sensitizers with similar structure and a series of Fc derivatives in search of the minimal driving force (Figure 10).[30] The threshold of driving force for achieving 99.9% regeneration efficiency is determined as 0.20−0.25 eV.

Interestingly, Figure 10b indicates that the regeneration rate is chiefly dominated by the driving force, while the electron coupling constants depending on the architecture of the dye and the steric bulk of the redox couple appear to have less influence on the regeneration kinetics. Furthermore, the regeneration kinetics of Fc derivatives is in the normal Marcus region as the driving force is below 0.35 V. The inverted Marcus region of over 0.35 eV was not observed. This could be understood as the diffusion limitation inside TiO_2 film, or uneasy accessibility of the anchoring dyes owing to aggregation.[30] In this situation, the rate-determinant step in regeneration is the sluggish diffusion of Fc derivatives to the sensitizer cations.

Compared with Fc/Fc^+ couples, cobalt-complex shuttles show slower regeneration kinetics. It is known that Co(II) complexes have two low-lying electronic states, that, is the low-spin (LS) doublet states $(t_{2g})^6/(e_g)^1$ and the high-spin (HS) quartet states $(t_{2g})^5/(e_g)^2$. DFT calculations revealed that Co(II) complex such as $[Co(bpy)_3]^{2+}$ at low spin state rather than high spin state prefers to exchange electrons with the oxidized dyes because of relative lower activation barrier.[31] The sluggish regeneration by Co(II) complexes is hence attributed to the large inner-sphere reorganization energy for HS-LS transition. To lower down the activation barrier, a new motif of low-spin cobalt complexes $[Co(cctn)_2]^{2+/3+}$ was developed, which shows the self-exchange rate constant over $[Co(bpy)_3]^{2+/3+}$ by 4 orders of magnitude.[32] In this way, a driving force of 0.2 eV was confirmed to be sufficient to quantitative regeneration.

It is notable that the regeneration reactions for most of cobalt redox couples also occurred in normal Marcus region.[9] The architectures of the ligands of cobalt complexes appear to have no effect on the reorganization energy, in agreement with the observations on Fc derivatives. In addition, Figure 11 displays the plots of halftime and η_{reg} against the driving force. It reflects that a

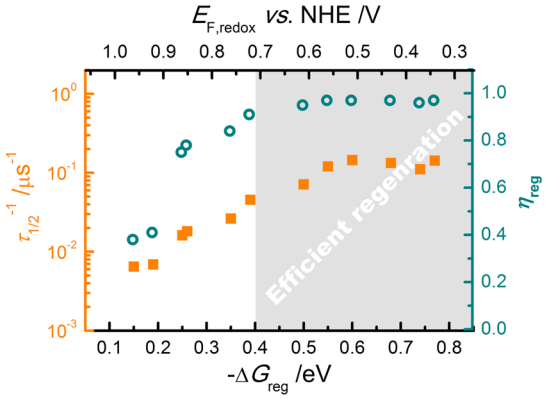

Figure 11. Plots of halftime and regeneration efficiency as a function of driving force. Experimental data for the plots are collected from ref 9 with permission from Royal Chemical Society.

driving force over 0.4 eV is sufficient to efficient regeneration with 0.1 M Co(II) complex. Feldt et al. also showed that the driving force of 0.25 eV for $[Co(bpy\text{-}pz)_2]^{2+}$ will become sufficient when its concentration is raised by four times. This means that the insufficient driving force could be partly compensated by raising the concentration of the reduced species (albeit under the limitation of dissolubility). Moreover, it is valuable to note that the regeneration efficiency also depends on the recombination rate constant of the dye cations. For example, the regeneration efficiency is relatively high (93%) for Y123 dye even for cobalt complexes $[Co(bpy\text{-}pz)_2]^{2+/3+}$ with a low driving force for regeneration (0.23 eV).[6]

Organic redox couples such as $TMTU/[TMFDS]^{2+}$ and T^-/T_2 exhibit less efficient kinetics in dye regeneration reaction compared with the iodine counterpart. In DSCs with dye Z907, the halftime of regeneration for $TMTU/[TMFDS]^{2+}$ based mediators is about 3 times longer than the iodine-based electrolytes.[17] This is mainly attributed to more positive redox potential of $TMTU/[TMFDS]^{2+}$, which reduces the driving force by 0.22 eV. However, the regeneration efficiency could be enhanced from 43% to 93% when sensitizer Z907 is replaced by organic dye D131 associated with relative lower HOMO level. For DSCs with T^-/T_2 redox mediators, regeneration efficiency is shown to be improved by introducing lithium ions into electrolyte.[16] Note that the intercalation of lithium cations at the surfaces of TiO_2 plays a role in promoting the accumulation of T^-. Similar phenomena have also been observed in iodine-based DSCs.

4. CONCLUSION

Deep understanding of the electron transfer kinetics is vital to make a new breakthrough in the development of highly efficient iodine-free DSCs. Current knowledge of electron recombination and dye regeneration on metallorganic and organic sulfur redox couples has been summarized. For metallorganic redox shuttles featuring fast electron interception behavior, comprehensive surface engineering on TiO_2 film is required for retarding recombination. In comparison, sluggish charge transfer property of organic sulfur redox couples makes the cell performance highly dependent on dye regeneration efficiency. Note that a well-designed sensitizer is ultimate to make the best of these alternative redox couples. In addition, the architecture of the TiO_2 film as well as the energetics of the conduction band and bandgap states need to be tailored systematically for controlling electron recombination and dye regeneration.

DOI: 10.1021/ar500337g
Acc. Chem. Res. 2015, 48, 1541−1550

■ ASSOCIATED CONTENT

Supporting Information

Estimation on the losses of photovoltage and photocurrent by recombination, redox reaction of disulfide/thiolate redox couple (T^-/T_2). The Supporting Information is available free of charge on the ACS Publications website at DOI: 10.1021/ar500337g.

■ AUTHOR INFORMATION

Corresponding Author

*E-mail: chenabc@nankai.edu.cn.

Notes

The authors declare no competing financial interest.

Biographies

Zhe Sun received his Ph.D. in Chemical Engineering from Tianjin University in 2006. Currently, he is an associate professor at School of Chemistry & Chemical Engineering, Tianjin University of Technology, and a visiting professorial scholar at KLAEMC, Nankai University. His research interest focuses on kinetics of DSCs, particularly the processes of interfacial electron transfer.

Mao Liang received his Ph.D. in inorganic chemistry under the supervision of Prof. Jun Chen from Nankai University in 2007. He is presently an associate professor at Department of Applied Chemistry, Tianjin University of Technology, and a visiting professorial scholar at KLAEMC, Nankai University. His current research interest focuses on the design and synthesis of dye sensitizers for DSCs.

Chen Jun obtained his B.Sc. and M.Sc. degrees from Nankai University in 1989 and 1992, respectively, and his Ph.D. from Wollongong University (Australia) in 1999. He held the NEDO fellowship at National Institute of AIST Kansai Center (Japan) from 1999 to 2002. He was appointed as the Chair Professor of Energy Materials Chemistry at Nankai University in 2002, the Outstanding Young Scientist from NSFC in 2003, Cheung Kong Scholar from Ministry of Education in 2005, the Chief Scientist of the National Nano Key Science Research in 2010. His research expertise is energy conversion and storage with solar cells, fuel cells, and batteries.

■ ACKNOWLEDGMENTS

The support of the National Projects of 973 (2011CBA00702), NSFC (21103123 and 21373007), and MOE (IRT13R30 and B12015) is gratefully acknowledged.

■ REFERENCES

(1) O'Regan, B. C.; Grätzel, M. A Low-Cost, High-Efficiency Solar Cell Based on Dye-Sensitized Colloidal TiO_2 Films. *Nature* **1991**, *353*, 737−740.

(2) Liang, M.; Chen, J. Arylamine Organic Dyes for Dye-sensitized Solar Cells. *Chem. Soc. Rev.* **2013**, *42*, 3453−3488.

(3) Mathew, S.; Yella, A.; Gao, P.; Humphry-Baker, R.; Curchod, B. F.E.; Ashari-Astani, N.; Tavernelli, I.; Rothlisberger, U.; Nazeeruddin, Md. K.; Grätzel, M. Dye-Sensitized Solar Cells with 13% Efficiency Achieved through the Molecular Engineering of Porphyrin Sensitizers. *Nat. Chem.* **2014**, *6*, 242−247.

(4) Snaith, H. J. Estimating the Maximum Attainable Efficiency in Dye-Sensitized Solar Cells. *Adv. Funct. Mater.* **2010**, *20*, 13−19.

(5) Feldt, S. M.; Gibson, E. A.; Gabrielsson, E.; Sun, L.; Boschloo, G.; Hagfeldt, A. Design of Organic Dyes and Cobalt Polypyridine Redox Mediators for High-Efficiency Dye-Sensitized Solar Cells. *J. Am. Chem. Soc.* **2010**, *132*, 16714−16724.

(6) Yum, J. H.; Baranoff, E.; Kessler, F.; Moehl, T.; Ahmad, S.; Bessho, T.; Marchioro, A.; Ghadiri, E.; Moser, J. E.; Yi, C.; Nazeeruddin, M. K.; Grätzel, M. A Cobalt Complex Redox Shuttle for Dye-Sensitized Solar Cells with High Open-Circuit Potentials. *Nat. Commun.* **2012**, *3*, 631.

(7) Zhou, D.; Yu, Q.; Cai, N.; Bai, Y.; Wang, Y.; Wang, P. Efficient Organic Dye-Sensitized Thin-Film Solar Cells Based on the Tris(1,10-phenanthroline) Cobalt(II/III) Redox Shuttle. *Energy Environ. Sci.* **2011**, *4*, 2030−2034.

(8) Burschka, J.; Dualeh, A.; Kessler, F.; Baranoff, E.; Cevey-Ha, N.; Yi, C.; Nazeeruddin, M. K.; Grätzel, M. Tris(2-(1*H*-pyrazol-1-yl)pyridine) Cobalt(III) as p-Type Dopant for Organic Semiconductors and Its Application in Highly Efficient Solid-State Dye-Sensitized Solar Cells. *J. Am. Chem. Soc.* **2011**, *133*, 18042−18045.

(9) Feldt, S. M.; Lohse, P. W.; Kessler, F.; Nazeeruddin, M. K.; Grätzel, M.; Boschloo, G.; Hagfeldt, A. Regeneration and Recombination Kinetics in Cobalt Polypyridine Based Dye-Sensitized Solar Cells, Explained Using Marcus Theory. *Phys. Chem. Chem. Phys.* **2013**, *15*, 7087−7097.

(10) Ning, Z.; Fu, Y.; Tian, H. Improvement of Dye-Sensitized Solar Cells: What We Know and What We Need to Know. *Energy Environ. Sci.* **2010**, *3*, 1170−1181.

(11) Daeneke, T.; Kwon, T. H.; Holmes, A. B.; Duffy, N. W.; Bach, U.; Spiccia, L. High-Efficiency Dye-Sensitized Solar Cells with Ferrocene-Based Electrolytes. *Nat. Chem.* **2011**, *3*, 211−215.

(12) Bisquert, J. Dilemmas of Dye Solar Cells. *ChemPhysChem* **2011**, *12*, 1633−1636.

(13) Li, T. C.; Spokoyny, A. M.; She, C.; Farha, O. K.; Mirkin, C. A.; Marks, T. J.; Hupp, J. T. Ni(III)/(IV) Bis(dicarbollide) as a Fast, Noncorrosive Redox Shuttle for Dye-Sensitized Solar Cells. *J. Am. Chem. Soc.* **2010**, *132*, 4580−4582.

(14) Haring, A. J.; Pomatto, M. E.; Thornton, M. R.; Morris, A. J. $Mn^{II/III}$ Complexes as Promising Redox Mediators in Quantum-Dot-Sensitized Solar Cells. *ACS Appl. Mater. Interfaces* **2014**, *6*, 15061−15067.

(15) Apostolopoulou, A.; Vlasiou, M.; Tziouris, P. A.; Tsiafoulis, C.; Tsipis, A. C.; Rehder, D.; Kabanos, T. A.; Keramidas, A. D.; Stathatos, E. Oxidovanadium (IV/V) Complexes as New Redox Mediators in Dye-Sensitized Solar Cells: A Combined Experimental and Theoretical Study. *Inorg. Chem.* **2015**, *54*, 3979−3988.

(16) Wang, M.; Chamberland, N.; Breau, L.; Moser, J. E.; Humphry-Baker, R.; Marsan, B.; Zakeeruddin, S. M.; Grätzel, M. An Organic Redox Electrolyte to Rival Triiodide/Iodide in Dye-Sensitized Solar Cells. *Nat. Chem.* **2010**, *2*, 385−389.

(17) Liu, Y.; Jennings, J. R.; Wang, Q. Efficient Dye-Sensitized Solar Cells Using a Tetramethylthiourea Redox Mediator. *ChemSusChem* **2013**, *6*, 2124−2131.

(18) Tian, H.; Jiang, X.; Yu, Z.; Kloo, L.; Hagfeldt, A.; Sun, L. Efficient Organic-Dye-Sensitized Solar Cells Based on an Iodine-Free Electrolyte. *Angew. Chem., Int. Ed.* **2010**, *49*, 7328−7331.

(19) Yu, S.; Ahmadi, S.; Sun, C.; Palmgren, P.; Hennies, F.; Zuleta, M.; Göthelid, M. 4-tert-Butyl Pyridine Bond Site and Band Bending on TiO_2 (110). *J. Phys. Chem. C* **2010**, *114*, 2315−2320.

(20) Salim, N. T.; Yang, X.; Zhang, S.; Liu, J.; Islam, A.; Han, L. Shielding Effects of Additives in a Cobalt(II /III) Redox Electrolyte: toward Higher Open-Circuit Photovoltages in Dye-Sensitized Solar Cells. *J. Mater. Chem. A* **2014**, *2*, 10532−10539.

(21) Long, H.; Zhou, D.; Zhang, M.; Peng, C.; Uchida, S.; Wang, P. Probing Dye-Correlated Interplay of Energetics and Kinetics in Mesoscopic Titania Solar Cells with 4-*tert*-Butylpyridine. *J. Phys. Chem. C* **2011**, *115*, 14408−14414.

(22) Bakke, J. R.; Pickrahn, K. L.; Brennan, T. P.; Bent, S. F. Nanoengineering and Interfacial Engineering of Photovoltaics by Atomic Layer Deposition. *Nanoscale* **2011**, *3*, 3482−3508.

(23) Tien, T. C.; Pan, F.-M.; Wang, L. P.; Tsai, F. Y.; Lin, C. Coverage Analysis for the Core/Shell Electrode of Dye-Sensitized Solar Cells. *J. Phys. Chem. C* **2010**, *114*, 10048−10053.

(24) Chandiran, A. K.; Tetreault, N.; Humphry-Baker, R.; Kessler, F.; Baranoff, E.; Yi, C.; Nazeeruddin, M. K.; Grätzel, M. Subnanometer Ga_2O_3 Tunnelling Layer by Atomic Layer Deposition to Achieve 1.1 V Open-Circuit Potential in Dye-Sensitized Solar Cells. *Nano Lett.* **2012**, *12*, 3941−3947.

DOI: 10.1021/ar500337g
Acc. Chem. Res. 2015, 48, 1541−1550

(25) Prasittichai, C.; Avila, J. R.; Farha, O. K.; Hupp, J. T. Systematic Modulation of Quantum (Electron) Tunneling Behavior by Atomic Layer Deposition on Nanoparticulate SnO_2 and TiO_2 Photoanodes. *J. Am. Chem. Soc.* **2013**, *135*, 16328−16331.
(26) Mäkinen, V.; Honkala, K.; Häkkinen, H. Atomic Layer Deposition of Aluminum Oxide on TiO_2 and Its Impact on N3 Dye Adsorption from First Principles. *J. Phys. Chem. C* **2011**, *115*, 9250−9259.
(27) Docampo, P.; Tiwana, P.; Sakai, N.; Miura, H.; Herz, L.; Murakami, T.; Snaith, H. J. Unraveling the Function of an MgO Interlayer in Both Electrolyte and Solid-State SnO_2 Based Dye-Sensitized Solar Cells. *J. Phys. Chem. C* **2012**, *116*, 22840−22846.
(28) Brennan, T. P.; Tanskanen, J. T.; Roelofs, K. E.; To, J. W. F.; Nguyen, W. H.; Bakke, J. R.; Ding, I.-K.; Hardin, B. E.; Sellinger, A.; McGehee, M. D.; Bent, S. F. TiO_2 Conduction Band Modulation with In_2O_3 Recombination Barrier Layers in Solid-State Dye-Sensitized Solar Cells. *J. Phys. Chem. C* **2013**, *117*, 24138−24149.
(29) Li, F.; Jennings, J. R.; Wang, Q. Determination of Sensitizer Regeneration Efficiency in Dye-Sensitized Solar Cells. *ACS Nano* **2013**, *7*, 8233−8242.
(30) Daeneke, T.; Mozer, A.; Uemura, Y.; Makuta, S.; Fekete, M.; Tachibana, Y.; Koumura, N.; Bach, U.; Spiccia, L. Dye Regeneration Kinetics in Dye-Sensitized Solar Cells. *J. Am. Chem. Soc.* **2012**, *134*, 16925−16928.
(31) Mosconi, E.; Yum, J. H.; Kessler, F.; Gómez García, C. J.; Zuccaccia, C.; Cinti, A.; Nazeeruddin, M. K.; Grätzel, M.; De Angelis, F. Cobalt Electrolyte/Dye Interactions in Dye-Sensitized Solar Cells: A Combined Computational and Experimental Study. *J. Am. Chem. Soc.* **2012**, *134*, 19438−19453.
(32) Xie, Y.; Hamann, T. W. Fast Low-Spin Cobalt Complex Redox Shuttles for Dye-Sensitized Solar Cells. *J. Phys. Chem. Lett.* **2013**, *4*, 328−332.

DOI: 10.1021/ar500337g
Acc. Chem. Res. 2015, 48, 1541−1550